

# Extending the operation range of a phase-sensitive optical time-domain reflectometer by using fibre with chirped Bragg gratings

D.R. Kharasov, D.M. Bengalskii, M.Yu. Vyatkin, O.E. Nanii, E.A. Fomiryakov, S.P. Nikitin, S.M. Popov, Yu.K. Chamorovsky, V.N. Treshchikov

**Abstract.** A record long external-disturbance detection distance of 140 km without employing optical amplifiers in the fibre line is demonstrated by a phase-sensitive optical time-domain reflectometer ( $\Phi$ -OTDR) using a fibre section with inscribed chirped fibre Bragg gratings (CFBGs). This solution provides simultaneous operation of  $\Phi$ -OTDR with a standard single-mode fibre at a distance of up to 100 km and with a CFBG fibre section located from the fibre line input point by at least 140 km.

**Keywords:** distributed sensor, fibre-optic sensor, phase-sensitive optical reflectometer, coherent reflectometer, fibre Bragg gratings, chirped fibre Bragg gratings.

## 1. Introduction

Rayleigh phase-sensitive optical time-domain reflectometers ( $\Phi$ -OTDR,  $\phi$ OTDR, COTDR) [1–3] are widely used as distributed fibre sensors for monitoring and protecting extended objects. The  $\Phi$ -OTDR operation range is limited by light attenuation in a fibre and usually equals to  $\sim 50$  km.

There are several ways to make the operation distance of  $\Phi$ -OTDR longer. The first one is the employment of low-attenuation fibres. For example, the employment of a ULL-fibre with losses of  $\sim 0.16$  dB km<sup>-1</sup> instead of a standard single-mode fibre (SSMF) with losses of  $\sim 0.2$  dB km<sup>-1</sup> increases the  $\Phi$ -OTDR operation distance by 25%. If a power supply is available along the fibre line, then the operation distance can be increased by installing inline erbium-doped fibre amplifiers (EDFAs) [4]. Another approach is the employment of remote optical pumping amplifiers (ROPAs) and/or distributed Raman amplifiers [5, 6]. The employment of a conventional first-order distributed Raman amplifier with single-sided for-

ward pumping increases the  $\Phi$ -OTDR operation distance by approximately 30 km [7].

The third method for increasing the operation distance of the  $\Phi$ -OTDR is based on connecting fibres with subsequently increasing coefficients of Rayleigh scattering. For example, the three fibres connected in series were used in [8]: SSMF, nonzero dispersion-shifted fibre (NZDSF), and dispersion compensating fibre (DCF). The combined employment increased the operation distance of the  $\Phi$ -OTDR from 29 to 43 km. Since Rayleigh scattering is the main mechanism of light attenuation in a fibre, fibres with higher Rayleigh scattering coefficient possess, as a rule, higher attenuation.

One can increase the power of a detected optical signal ( $\Phi$ -OTDR trace) by using a fibre with inscribed Bragg gratings (FBGs). Light reflected from FBGs is totally transferred to a fibre mode, which is preferable as compared to Rayleigh scattering where only a small part of scattered radiation passes to the fibre mode. It was shown [9] that an amplitude of the  $\Phi$ -OTDR trace from a fibre section with FBGs [10, 11] is 150 times greater ( $\sim 22$  dB) than that of an ordinary fibre. However, a narrow reflection spectrum of ordinary FBGs hinders practical employment of the latter. Wang et al. [12] suggest using a fibre with ultraweak FBGs with a length of about 50  $\mu$ m. In spite of a lower reflection coefficient of such a FBG, the reflection spectrum is substantially wider ( $\sim 8$  nm) as compared to that of ordinary FBGs. Another way to expand the reflection spectrum is the employment of a fibre with inscribed chirped fibre Bragg gratings (CFBGs) [13]. Since both ultraweak and chirped gratings provide an expanded reflection spectrum, the choice of a particular solution is determined by the convenience of realisation with an employed technology available for grating fabrication, which provides the required device parameters. In [14], the fibre line comprised of an ULL fibre of length 120 km and a fibre with an OFS Acoustisens CFBG [15] of length 5 km has demonstrated coherent reflectometer operation without line amplifiers at a distance of 125 km. A  $\Phi$ -OTDR signal at the section 90–120 km was below the reflectometer noise level.

The aim of the present work is to demonstrate the possibility of  $\Phi$ -OTDR detection of a vibroacoustic action on the sections of CFBG fibre distant from the device position by more than 125 km along the cable line based on a SSMF telecommunication fibre of G-652 standard.

## 2. Materials and methods

For increasing the operation distance of a vibroacoustic sensor, we used a high-sensitive  $\Phi$ -OTDR ‘Dunai’ produced by

**D.R. Kharasov** T8 Sensor Ltd., Krasnobogatyrskaya ul. 44/1, 107076 Moscow, Russia; Moscow Institute of Physics and Technology, Institutskii per. 9, 141701 Dolgoprudnyi, Moscow region, Russia; e-mail: kharasov@phystech.edu;

**D.M. Bengalskii, O.E. Nanii, E.A. Fomiryakov** T8 Sensor Ltd., Krasnobogatyrskaya ul. 44/1, 107076 Moscow, Russia; Lomonosov Moscow State University, Vorob’evy gory, 119991 Moscow, Russia; **M.Yu. Vyatkin, S.M. Popov, Yu.K. Chamorovsky** Kotel’nikov Institute of Radio Engineering and Electronics (Fryazino Branch), Russian Academy of Sciences, pl. Vvedenskogo 1, 141190 Fryazino, Moscow region, Russia;

**S.P. Nikitin, V.N. Treshchikov** T8 Sensor Ltd., Krasnobogatyrskaya ul. 44/1, 107076 Moscow, Russia

Received 19 December 2019

*Kvantovaya Elektronika* 50 (5) 510–513 (2020)

Translated by N.A. Raspopov

T8 Sensor Ltd. [16] and test samples of a CFBG fibre produced by the Fryazino branch of IRE RAS [17]. The CFBG fibre parameters are as follows: the average linear density of gratings is  $2\text{ m}^{-1}$  and average grating length is 1 cm. A reflection spectrum of a single CFBG measured by a high-resolution optical frequency-domain reflectometer (OFDR) LUNA OBR 4400 is shown in Fig. 1. The maximum reflection is observed in the wavelength range 1550.2–1553.5 nm. Total losses in splices between SSMF and CFBG fibre measured by an optical time-domain reflectometer Anritzu MU90901515C6 were 4.3 dB.

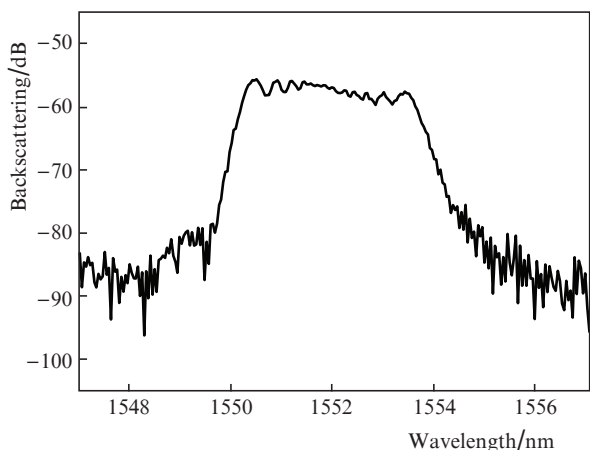


Figure 1. Reflection spectrum of an individual CFBG measured by using an OFDR-reflectometer LUNA OBR 4400.

A scheme of the experimental setup is given in Fig. 2. A nearly square shape probe pulse of duration  $\tau_p = 200\text{ ns}$  with a pulse repetition rate  $f_s = 500\text{ Hz}$  was formed in a  $\Phi$ -OTDR from cw output of a narrow-linewidth single-frequency laser with a wavelength of 1550.12 nm by an acousto-optical modulator. The probe pulse was amplified to 150 mW by an EDFA booster. The pulse power from a 1%-output of fused coupler was measured by a Thorlabs DET01CFC photodetector connected to an Agilent Infinium DSA90804A oscillo-

scope. The  $\Phi$ -OTDR was connected to a fibre line formed by three fibres connected in series: SSMF of length 140 km, CFBG fibre of length 300 m, and SSMF of length 30 km. The fibre line average attenuation is  $\alpha = 0.185\text{ dB km}^{-1}$ . The whole fibre line was located on an active pneumatic vibration isolation table, and fibre spools were placed in soundproofing foam-rubber boxes. A backscattered optical signal passed through a circulator to the input of an EDFA pre-amplifier for additional amplification. The amplified optical signal was detected by an optical-to-electrical converter (O/E) and then digitised by an analogue-to-digital converter (A/D). A field-programmable gate array (FPGA) was used to transfer  $\Phi$ -OTDR data to a computer for further signal processing.

The time dependence of the O/E photocurrent corresponds to the dependence of the backscattered optical power on the delay time  $\tau_d$  relative to the time moment of injecting a probe pulse into the fibre line. This delay time is related with a distance along the fibre:  $z = v_g \tau_d / 2$ , where  $v_g$  is the group velocity in the fibre line. The maximal usable fibre line length is limited by the probe pulse rate  $f_s$  and equals  $z_{\text{max}} = v_g / (2f_s) = 200\text{ km}$ . In addition,  $\Phi$ -OTDR traces were measured under the external acoustic disturbances produced by a speaker connected to a source of the sinusoidal signal at 502 Hz.

### 3. Experimental results

Figure 3 shows a  $\Phi$ -OTDR trace on a logarithmic scale, namely, the dependence of the optical power of the  $\Phi$ -OTDR trace on the distance  $z$  along the fibre. The  $\Phi$ -OTDR trace looks like a jagged curve. The  $\Phi$ -OTDR intrinsic noise is about  $-46.7\text{ dB}$ . The average level of the  $\Phi$ -OTDR trace falls with the distance due to the attenuation of the probe pulse as the latter propagates in the straight direction and to attenuation of the backscattered optical signal propagating in the opposite direction. For estimating the average power level of the  $\Phi$ -OTDR, the  $\Phi$ -OTDR trace moving mean in a 200-m sliding window is shown. A linear approximation is also presented for the average power on a logarithmic scale as a function of a distance along the fibre line. As expected, the slope of the obtained dependence coincides to a high

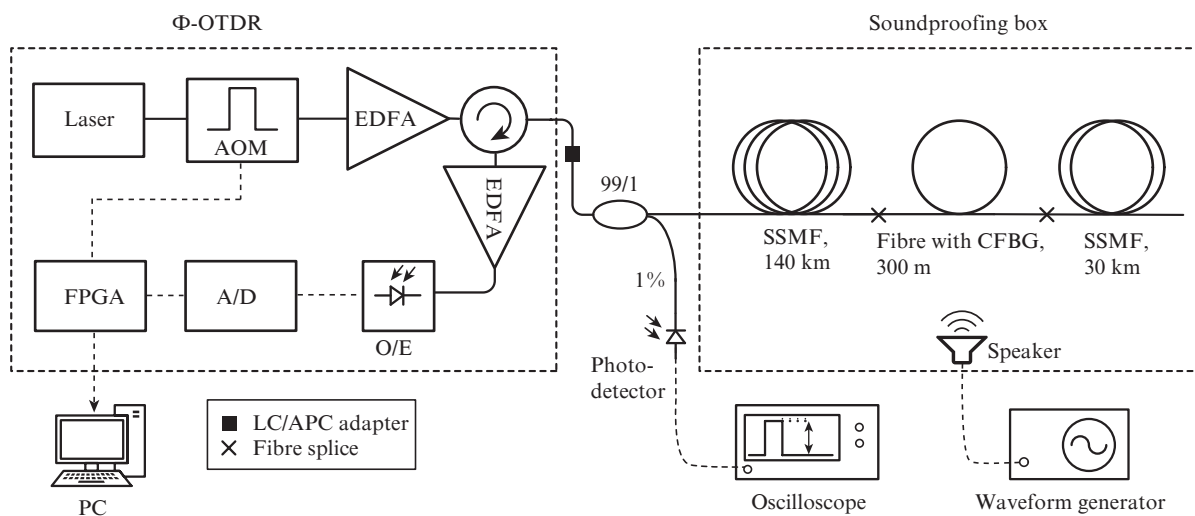
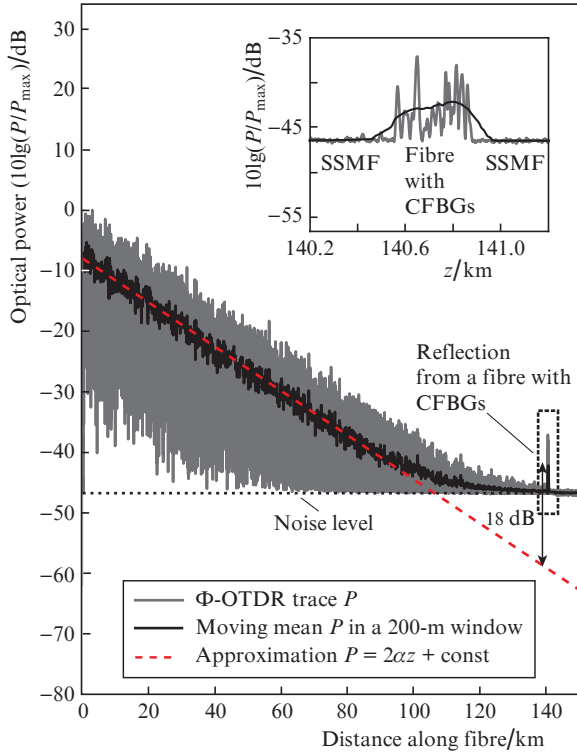


Figure 2. Experimental setup with a 170-km fibre line. The CFBG fibre of length 300 m is arranged at a distance of 140 km.



**Figure 3.**  $\Phi$ -OTDR trace in the logarithmic scale (black curve corresponds to the moving mean of the  $\Phi$ -OTDR trace within a 200-m sliding window, dashed curve is approximation of the average level). The inset shows a  $\Phi$ -OTDR trace from the fibre line section 140.2–141.2 km.

accuracy with the doubled average attenuation in fibre  $2\alpha$ . At first 50 km of the fibre line,  $\Phi$ -OTDR trace minima and maxima are above the noise level and well distinguished on it.

Starting from the 50th km, minima of the  $\Phi$ -OTDR trace are below the noise level and cannot be distinguished, whereas its average level coincides with the power level linear approximation within spikes to a distance of approximately 82 km. At longer distances, experimental measurements of the average level are incorrect, because a greater part of the  $\Phi$ -OTDR trace is below the intrinsic noise level. According to the linear approximation, the average level of the  $\Phi$ -OTDR trace reaches the intrinsic noise level near 106 km. In the section with CFBG fibre (140 km), the  $\Phi$ -OTDR trace is noticeably above the noise level: the running mean is above the noise level by approximately 4 dB and coincides with the theoretical level of the  $\Phi$ -OTDR trace corresponding to 90.5 km. The  $\Phi$ -OTDR trace moving mean for the CFBG fibre section is 18 dB above the theoretical average level of the  $\Phi$ -OTDR trace in SSMF fibre at the same distance (140 km).

Time dependence of the  $\Phi$ -OTDR signal (“waterfall”) in the fibre line section 140.2–141.2 km exposed to an external acoustic disturbance is shown in Fig. 4. One can see a  $\Phi$ -OTDR response to the external disturbance in the CFBG fibre section. In the general case, the response signal is nonlinear with respect to an external disturbance. The  $\Phi$ -OTDR signal from the section 140.77 km where the linear response is observed is shown in Fig. 5. The  $\Phi$ -OTDR signal was additionally processed using the 5th-order Butterworth filter with a 1–75 Hz passband. The  $\Phi$ -OTDR signal from the section 140.77 km is presented by a noisy sinusoidal curve at a frequency of 2 Hz with an amplitude of  $\pm 0.35$  a.u. The fre-

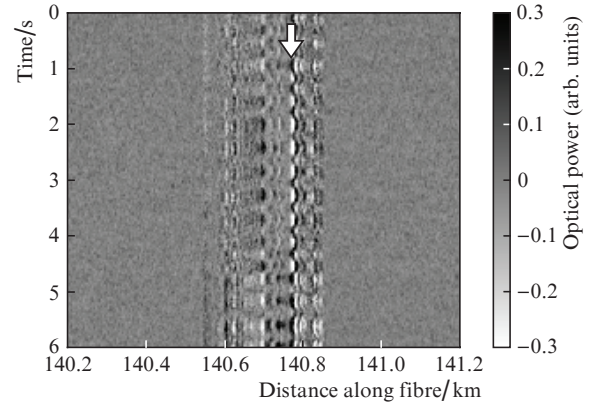


**Figure 4.** Time dependence of the  $\Phi$ -OTDR signal (“waterfall”) in the fibre line section 140.2–141.2 km. The arrow marks the fibre section with CFBGs at a distance of 140.77 km where the linear response to an external disturbance is observed.

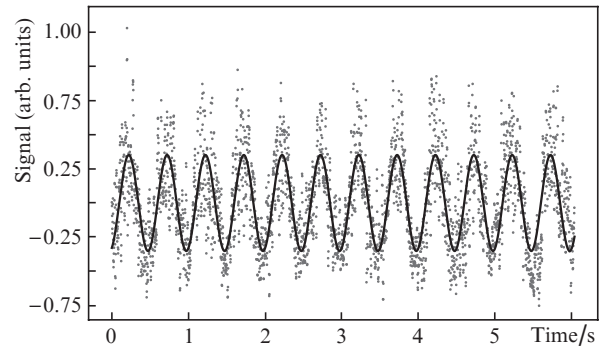


**Figure 5.** Time dependence of the  $\Phi$ -OTDR signal after filtering at the position of the CFBG fibre at a distance of 140.77 km where the linear response to an external disturbance is observed (solid curve is approximation by the function  $0.35\sin(2\pi \cdot 2t)$ ).

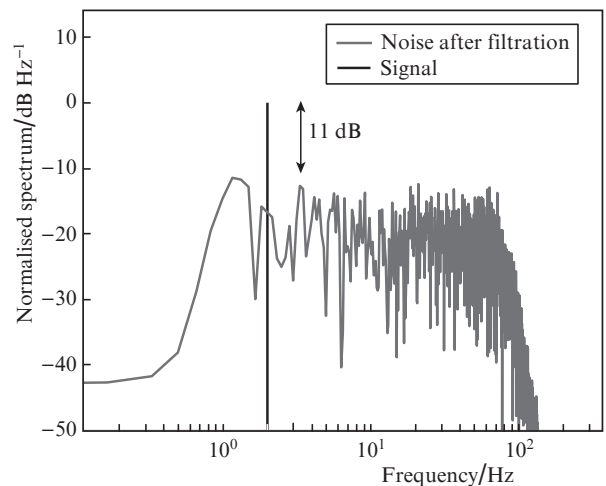


**Figure 6.** Spectrum normalised to the signal power and the band of 1 Hz at the position of the CFBG fibre at a distance of 140.77 km where the linear response to an external disturbance is observed.

quency of 2 Hz is due to the aliasing of the acoustic signal frequency probed at the pulse rate  $f_s = 500$  Hz. The standard deviation of the  $\Phi$ -OTDR data from the approximation curve is 0.22 a.u. Figure 6 presents the power spectrum of

noise obtained by discrete Fourier transformation, normalised to the signal power and bandwidth of 1 Hz. One can see that the noise level in the 1-Hz band is below the signal value by more than 11 dB.

Thus, the work has demonstrated a record long distance for the  $\Phi$ -OTDR detection of an external disturbance on a fibre section distant from the line starting point by 140 km without employing inline, remote and distributed optical amplifiers. The total attenuation covered by the  $\Phi$ -OTDR, which is equal to the attenuation distance multiplied by specific attenuation is 25.9 dB. With a ULL-type fibre possessing losses of  $\sim 0.16$  dB km<sup>-1</sup>, the  $\Phi$ -OTDR operation distance will be  $\sim 162$  km.

**Acknowledgements.** The sample of a fibre with CFBGs was fabricated by the Fryazino Branch of IRE RAS as part of a state assignment.

## References

1. Shatalin S.V., Treshchikov V.N., Rogers A. *J. Appl. Opt.*, **37** (24), 5600 (1998).
2. Hartog A.H. *Introduction to Distributed Optical Fibre Sensors* (Boca Raton: CRC press, 2017).
3. Alekseev A.E., Vdovenko V.S., Gorshkov B.G., Potapov V.T., Simikin D.E. *Laser Phys.*, **24** (11), 115106 (2014).
4. Tian X. et al. *Proc. SPIE, Optical Communication, Optical Fiber Sensors, and Optical Memories for Big Data Storage*, 10158, 101580P (2016); <https://doi.org/10.1117/12.2246763>.
5. Wang Z.N., Fan M.Q., Zhang L., Wu H., Li Y., Qian X.Y., Rao Y.J., Churkin D.V. *Opt. Express*, **23** (12), 15514 (2015).
6. Martins H.F., Martín-López S., Corredera P., Filograno M.L., Frazão O., Gonzalez-Herráez M. *J. Lightwave Technol.*, **32** (8), 1510 (2014).
7. Kharasov D.R. et al. *Proc. ICLO* (St. Petersburg, 2018) p. 285.
8. Nesterov E.T., Treshchikov V.N., Ozerov A.Zh., Sleptsov M.A., Kamynin V.A., Nanii O.E., Sus'yan A.A. *Pis'ma Zh. Tekh. Fiz.*, **37** (9), 55 (2011).
9. Ulanovskii F.I., Kuz'menkov A.I., Nanii O.E., Nikitin S.P., Treshchikov V.N. *Foton-ekspress*, **6** (126), 189 (2015).
10. Popov S.M. et al. *Proc. PIERS* (St. Peterburg, 2018) pp 1568–1573.
11. Zaitsev I.A., Butov O.V., Voloshin V.V., et al. *Radiotekh. Elektron.*, **61** (6), 602 (2016).
12. Wang X. et al. *IEEE Photonics J.*, **7** (1), 6800511 (2015); doi: 10.1109/JPHOT.2015.2396010.
13. Westbrook P.S. et al. *Proc. OFS* (Jeji, 2018) pp 1–5.
14. Cedilnik G. et al. *IEEE Sensors Lett.*, **3** (3), 1 (2019).
15. Handerek V.A. et al. *Proc. Optical Fiber Sensors* (Lausanne, 2018) p. TuC5.
16. Nikitin S.P., Kuzmenkov A.I., Gorbulyenko V.V., Nanii O.E., Treshchikov V.N. *Laser Phys.*, **28** (8), 085107 (2018).
17. Popov S.M., Butov O.V., Kolosovskii A.O. *Quantum Electron.*, **49** (12), 1127 (2019) [*Kvantovaya Elektron.*, **49** (12), 1127 (2019)].